

## Supplementary Information

### **Polydopamine Decorated MoS<sub>2</sub> Nanosheets based Electrochemical Immunosensor for Sensitive Detection of SARS-CoV-2 Nucleocapsid Protein in Clinical Samples**

Shalu Yadav<sup>1,2</sup>, Mohd. Abubakar Sadique<sup>1,2</sup>, Pushpesh Ranjan<sup>1,2</sup>, Raju Khan<sup>1,2\*</sup>, N. Sathish<sup>1,2</sup>, and Avanish K. Srivastava<sup>1,2</sup>

<sup>1</sup>CSIR – Advanced Materials and Processes Research Institute (AMPRI), Hoshangabad Road, Bhopal - 462026, India

<sup>2</sup>Academy of Scientific and Innovative Research (AcSIR), Ghaziabad - 201002, India

\*Corresponding author email: [khan.raju@gmail.com](mailto:khan.raju@gmail.com)

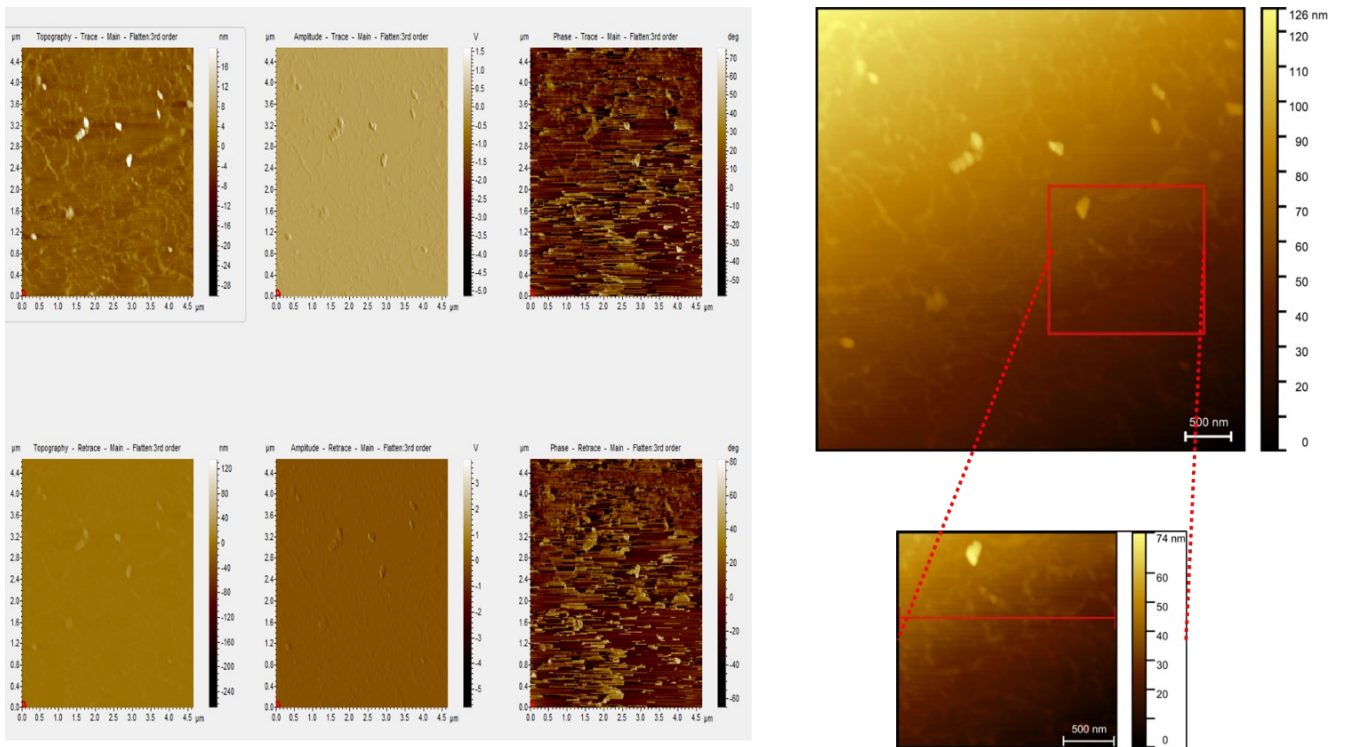


**Fig. S1** AFM images and selected area for analysis of MoS<sub>2</sub> NSs

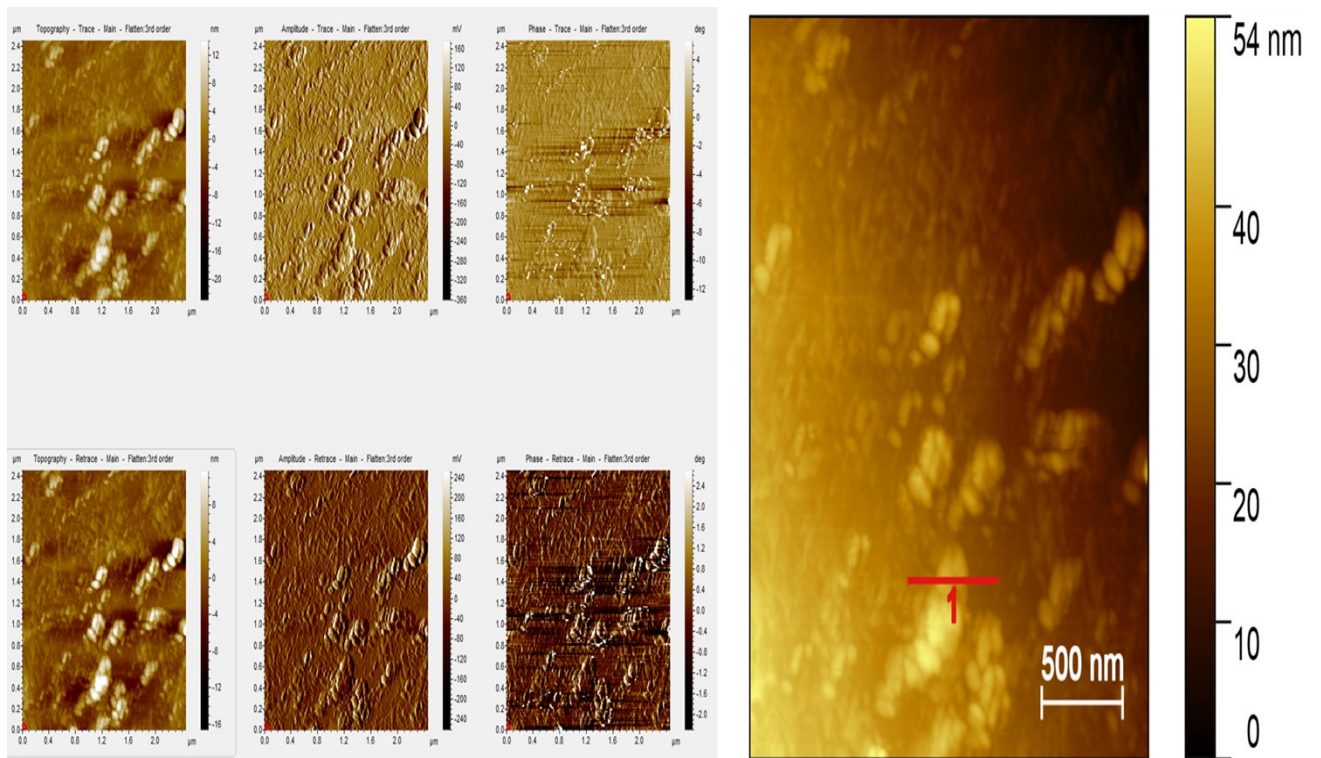


**Fig. S2** AFM images and selected area for analysis of MoS<sub>2</sub>-PDA nanocomposite

The  $R_{CT}$  values for electrode-modified surfaces were calculated from the Nyquist plot using the equation-

$$R_{CT} = R_p - R_s \quad (S1)$$

Where  $R_s$  is the solution resistance of electrolyte and  $R_p$  is the polarization resistance.

**Fig. S3** and **Fig. S4** show bode plots that demonstrate the relation between the frequency with the phase shift and amplitude respectively. The phase shift v/s frequency bode plot (**Fig. S3**) depict the different phase value recorded at a frequency value of  $\sim 1000$  Hz. The modified electrodes having a maximum phase shift below  $90^\circ$  attributed to the frequency where the resistance of electrodes mainly controlled the impedance. In **Fig. S4**, at low frequencies, the impedance relates the electron transfer process with mass transfer at the electrode surface. The rate of reaction can be determined by the frequency and impedance relation from the bode plots.<sup>1,2</sup>

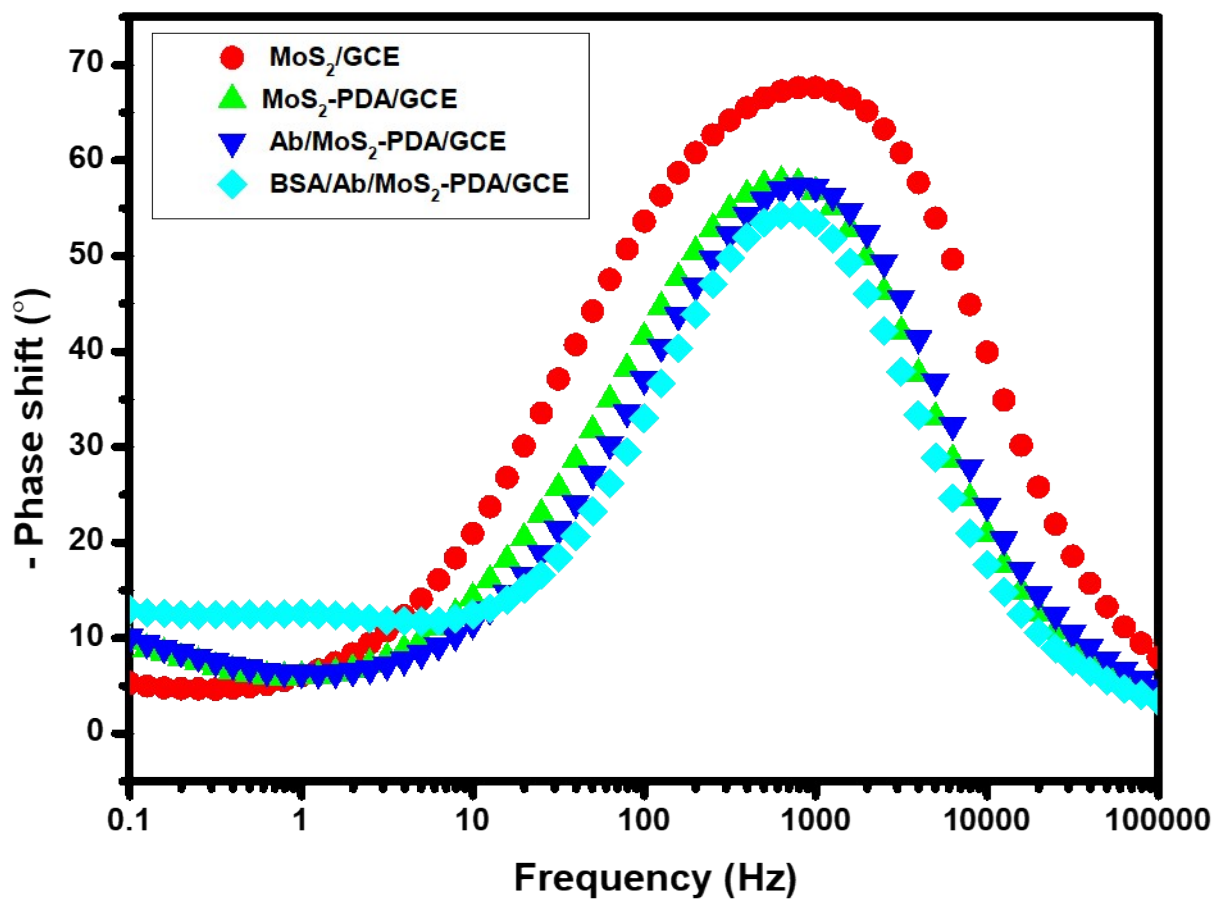


Fig. S3: Phase shift vs frequency plot after each step of surface-modified electrodes

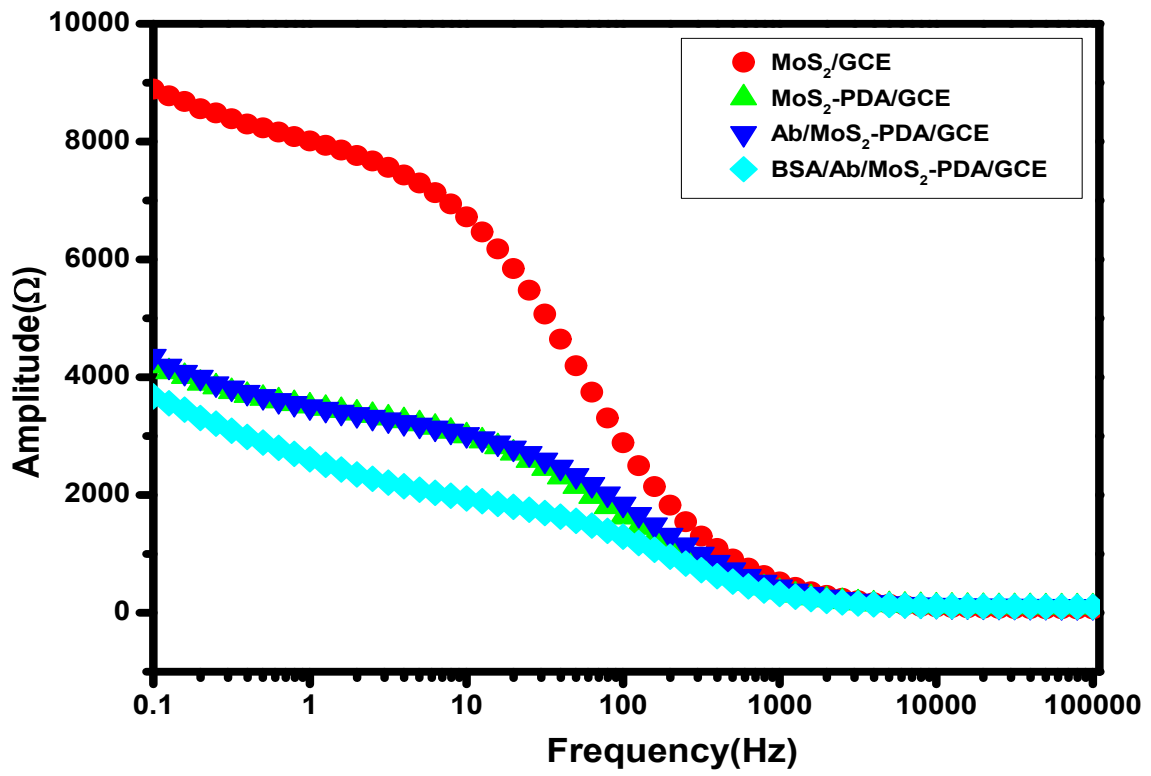
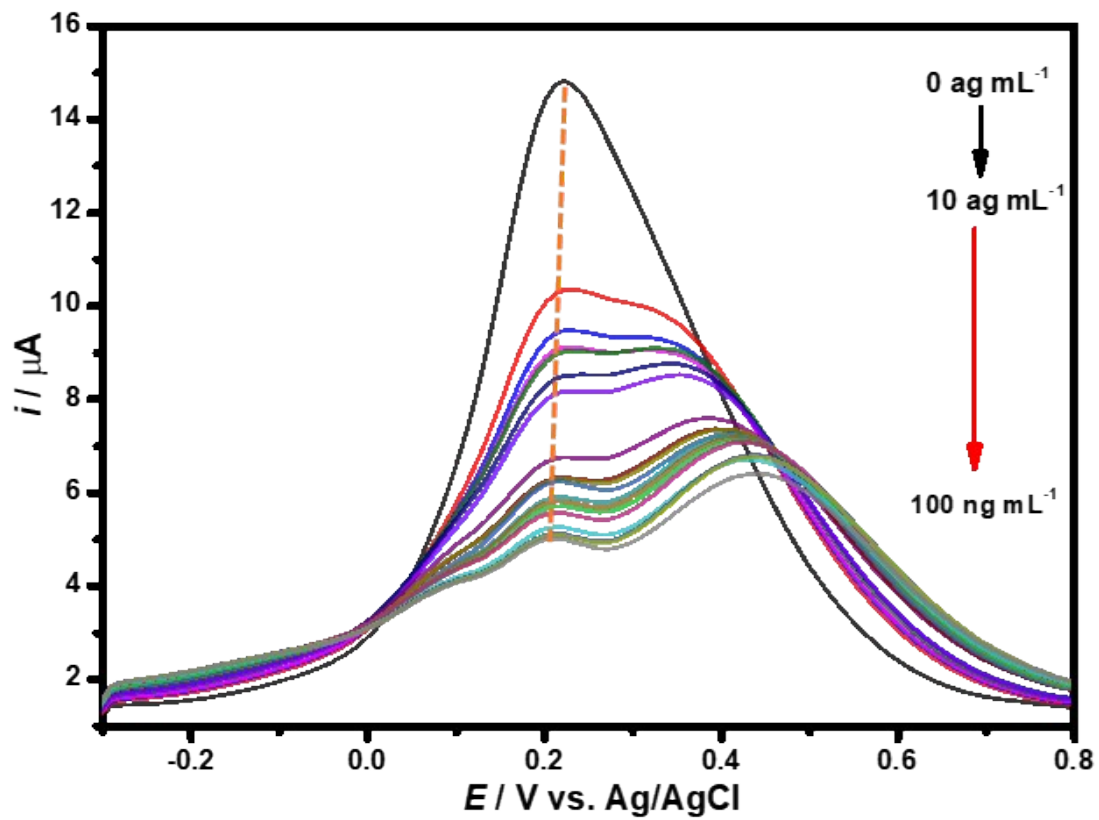


Fig. S4: Amplitude vs frequency plot after each step of surface-modified electrodes

### **Differential pulse voltammetry based detection of SARS-CoV-2 N protein**

Under optimal electrochemical conditions, an immunosensor was employed to detect N Protein via DPV. The immunosensor was incubated with different concentrations of N Protein ( $10 \text{ ag mL}^{-1}$  to  $100 \text{ ng mL}^{-1}$ ) in the redox electrolyte solution. The obtained peak current values are inversely proportional to the increasing concentration of N Protein as observed in the DPV curve at potential  $0.22 \text{ V}$ . (**Fig. S5**). The sharp decrease in immunosensor response current with the increase in the respective concentration of N Protein is attributed to the hindrance of electron transfer due to the formation of the Ab-N Protein complex on the electrode surface.<sup>3</sup> The linear regression curve analysis as shown in **Fig. S6** provided the immunosensor response i.e., change in peak current in DPV analysis for the concentration range from  $10 \text{ ag mL}^{-1}$  to  $100 \text{ ng mL}^{-1}$ .



**Fig. S5:** DPV detection curve of the immunosensor for the detection of different concentrations of N Protein ranging from  $10 \text{ ag mL}^{-1}$  to  $100 \text{ ng mL}^{-1}$ .



### Electrochemical immunosensor current response for SARS-CoV-2 N protein

The electrochemical immunosensor response was calculated based on the change percentage of the DPV peak current signals obtained for different N Protein concentrations ranging from 10 ag mL<sup>-1</sup> to 100 ng mL<sup>-1</sup> calculated from the following equation S2 -

$$\text{Immunosensor response } (\Delta i\%) = \frac{i_{\text{protein}} - i_0}{i_0} \times 100 \quad (\text{S2})$$

where  $\Delta i$  is the change in percentage of immunosensor response with increasing concentration of N Protein in the redox electrolyte solution,  $i_{\text{protein}}$  is the current obtained after incubating the immunosensor in N Protein, and  $i_0$  is the current obtained without N Protein in the redox electrolyte solution. The calibration plot between the  $\Delta i\%$  values and the logarithm of the concentration of N Protein along with the linearity equation:  $\Delta i = 3.6224 \text{ Log C (ag mL}^{-1}\text{)} + 29.72$  and its corresponding  $R^2 = 0.94761$  is shown in **Fig. S6**.

Furthermore, LOD and LOQ are calculated by the following equations (S3) and (S4) respectively-

$$LOD = \frac{3.3 \times SD}{S}, \quad (\text{S3})$$

$$LOQ = \frac{10 \times SD}{S}, \quad (\text{S4})$$

Where SD is the standard deviation of the response of the calibration curve = Standard error (SE) of intercept  $\times \sqrt{N}$ ,  $N$  = number of samples,  $S$  = Slope of the calibration curve. The obtained values of LOD and LOQ are **4.8 ag mL<sup>-1</sup>** and **14.53 ag mL<sup>-1</sup>** respectively.

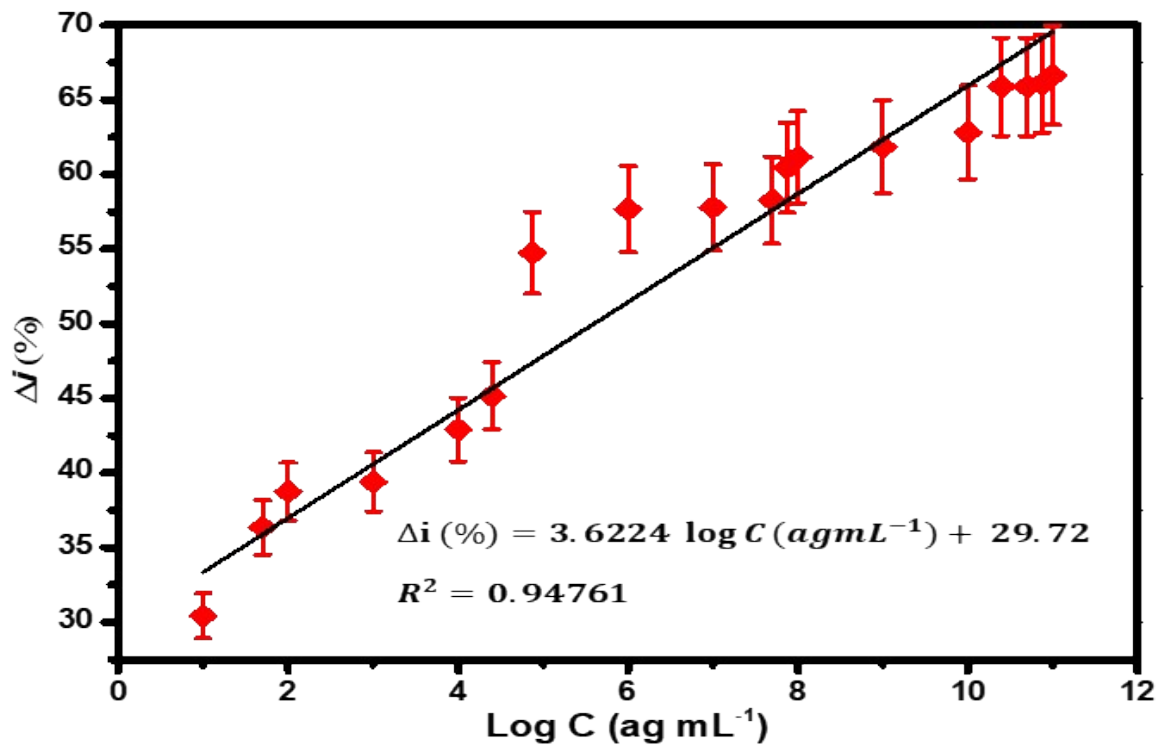


**Fig. S6:** The calibration curve of the immunosensor for the detection of different concentrations of N Protein ranging from 10 ag mL<sup>-1</sup> to 100 ng mL<sup>-1</sup>.

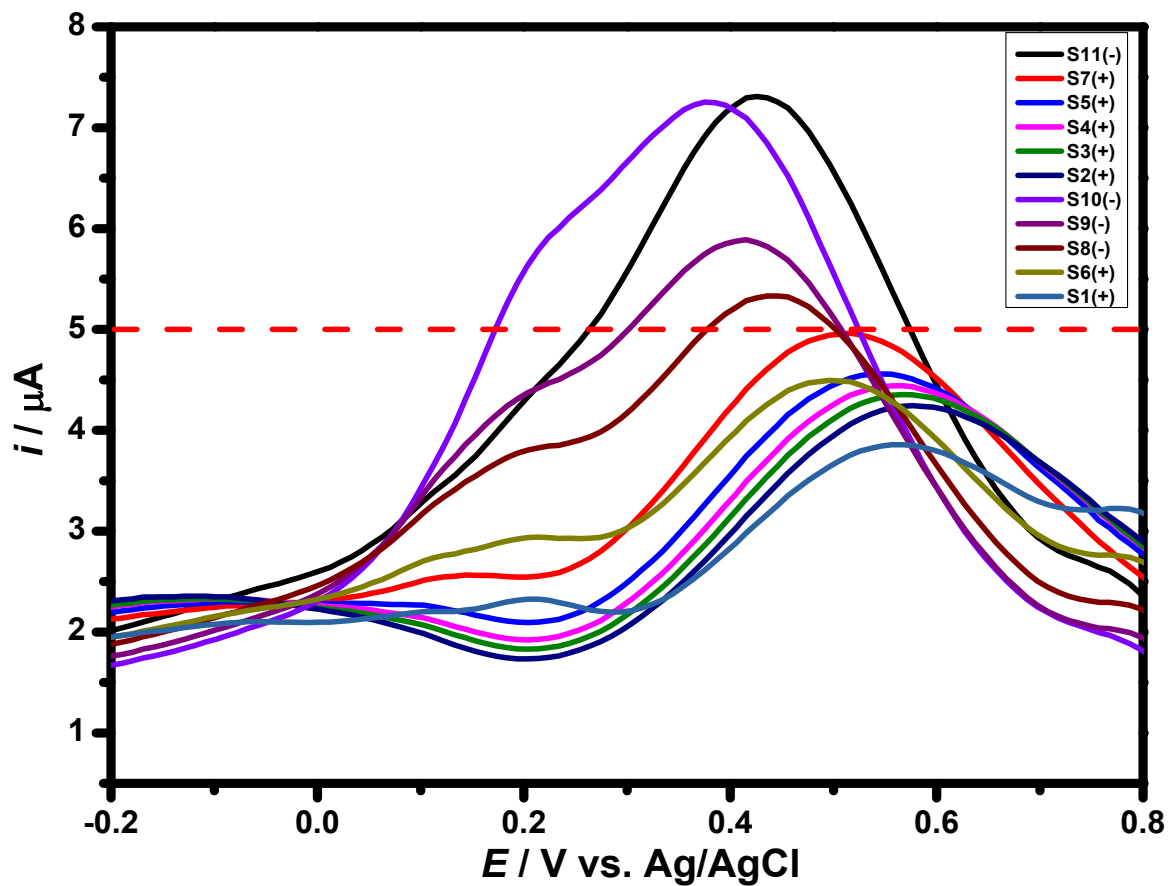


**Fig. S7:** Electrochemical immunosensor performance in nasopharyngeal swab samples of negative and positive patients through DPV<sup>4,5</sup>

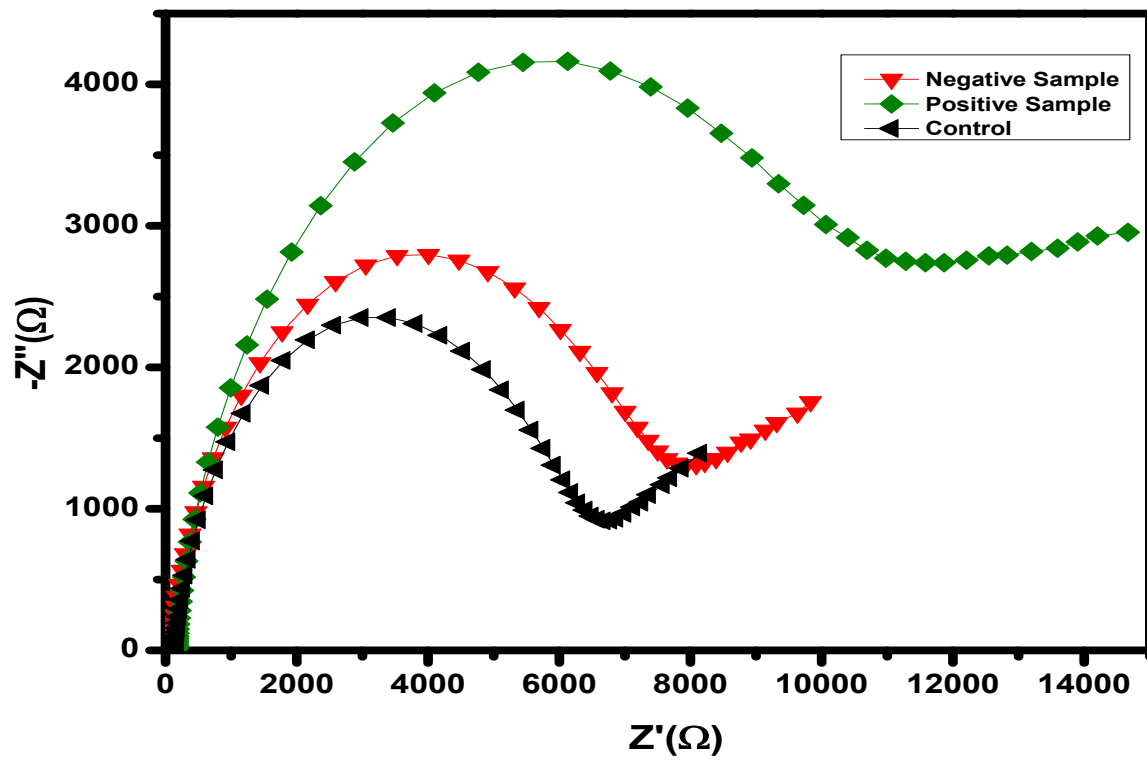
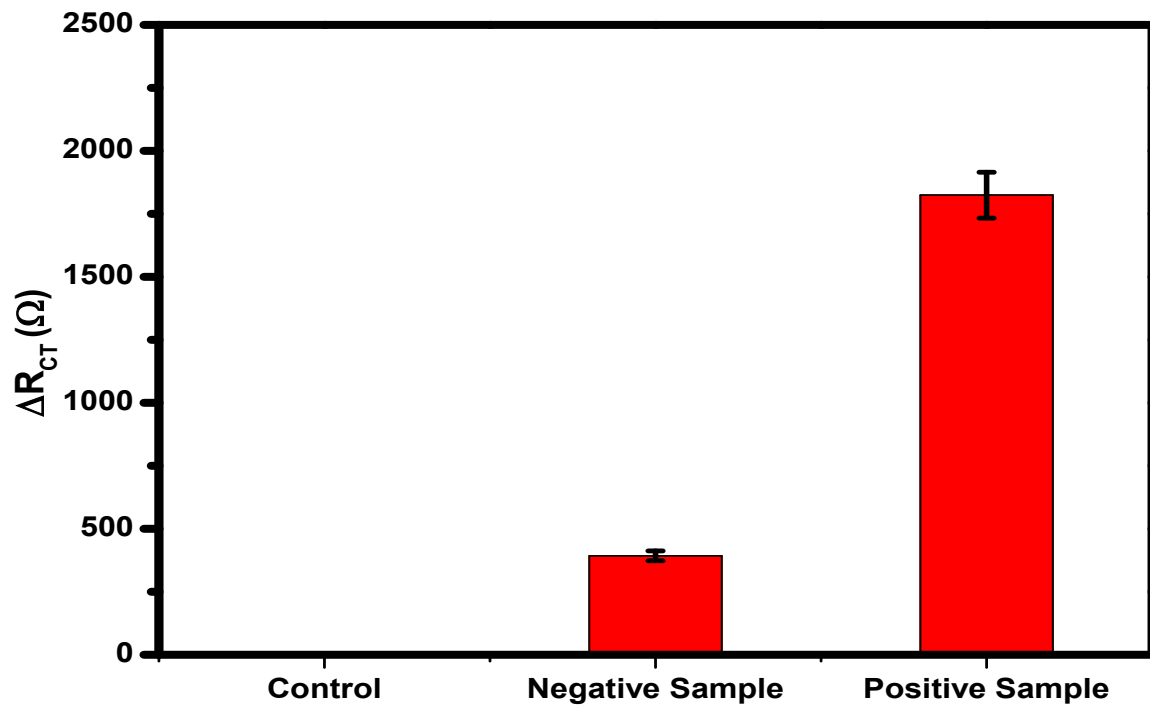


Fig. S8. Comparative Nyquist plot for negative and positive nasopharyngeal swab samples



**Fig. S9.** Comparative bar graph for negative and positive nasopharyngeal swab samples *via* EIS

## References

- 1 M. Drobysh, V. Liustrovaite, A. Baradoke, A. Rucinskiene, A. Ramanaviciene, V. Ratautaite, R. Viter, C.-F. Chen, I. Plikusiene, U. Samukaite-Bubniene, R. Slibinskas, E. Ciplys, M. Simanavicius, A. Zvirbliene, I. Kucinskaite-Kodze and A. Ramanavicius, *International Journal of Molecular Sciences*, 2022, **23**, 6768.
- 2 L. R. G. Silva, J. S. Stefano, L. O. Orzari, L. C. Brazaca, E. Carrilho, L. H. Marcolino-Junior, M. F. Bergamini, R. A. A. Munoz and B. C. Janegitz, *Biosensors*, 2022, **12**, 622.
- 3 Z. Rahmati, M. Roushani, H. Hosseini and H. Choobin, *Microchem J*, 2021, **170**, 106718.
- 4 L. F. de Lima, A. L. Ferreira, M. D. T. Torres, W. R. de Araujo and C. de la Fuente-Nunez, *Proceedings of the National Academy of Sciences*, 2021, **118**, e2106724118.
- 5 A. Yakoh, U. Pimpitak, S. Rengpipat, N. Hirankarn, O. Chailapakul and S. Chaiyo, *Biosens Bioelectron*, 2021, **176**, 112912.